Enhancement of thermoelectric properties in high mobility organic semiconductor, small molecule additive, and dopant composites

Stephen J. Lee, Jasmine Sinha, and Howard E. Katz

Department of Materials Science and Engineering
Johns Hopkins University
Baltimore, MD 21218, USA

I. Introduction

By directly converting heat flows into clean electricity, solid-state thermoelectric (TE) materials have the potential to help address our energy challenges. These heat flows result from temperature gradients that may be derived from solar and geothermal sources, as well as from inefficiencies in the existing energy framework. TE materials also have potential applications in battery-free electronics and can be run in reverse as refrigeration systems. Although polymer materials for TE applications have lower conversion efficiencies than their inorganic counterparts, they have potential applications due to their mechanical flexibility, light weight, and ability to be affordably solution-processed.

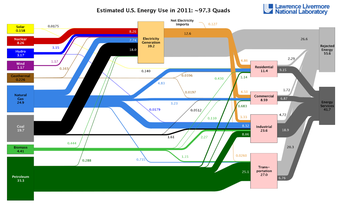

Fig. 1. More than 50% of the energy produced in the U.S. is never utilized; the majority of it is lost as waste heat

II. Background

Much of the current work in TE materials research involves increasing the TE figure of merit, ZT, conferring increased conversion efficiencies in cooling and in power generation.

$$ZT = S^2\sigma T/\kappa \qquad (1)$$

In this equation, S is the Seebeck coefficient, σ is the electrical conductivity, T is the average device temperature, and κ is the thermal conductivity. S is defined as the electrostatic potential across a material with a temperature difference; it is a measure of a property called the Seebeck effect which arises when charge carriers in the hot end of a material are excited and build-up. When this happens, an equilibrium forms between the electrostatic repulsion of these charges and the chemical potential for charge carrier diffusion to the cold end of the material. This interaction produces a potential difference and current.

$$S = \Delta V/\Delta T \qquad (2)$$

The main challenge regarding the optimization of OSCs as TE materials is the widely observed S-σ tradeoff. This is due to the fact that high S depends on the conductivity of charge carriers away from the Fermi level, ε_f, while high σ depends on the conductivity of charge carriers close to ε_f. By adding dopants to high mobility OSCs, σ is expected to increase due to the addition of mobile charge carriers. By introducing small molecule additives, S is expected to increase as carrier energy levels are introduced away from those of the bulk. When analyzing the S-σ tradeoff and ZT, a key metric is the Power Factor. All else being equal, increases in this quantity results in increases in the TE conversion efficiency of a conductor or semiconductor.

$$Power\ Factor = S^2\sigma \qquad (3)$$

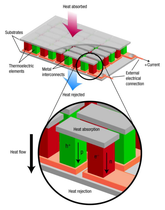

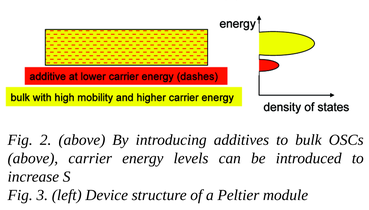

Fig. 2. (above) By introducing additives to bulk OSCs (above), carrier energy levels can be introduced to increase S
Fig. 3. (left) Device structure of a Peltier module

III. Design

The design component of the project involved choosing three component material systems of high mobility polymers, dopants, and small molecule additives. The high mobility polymers and dopants are intended to produce OSCs with high σ, and the additives are intended to modulate or increase S. PBTTT-C14 and CDT-BTZ-C16 were chosen because of their recent status as record high mobility polymers and the functionality of their simple thiophene units. F_4TCNQ and $NOPF_6$ were chosen because of their previous success as p-type dopants for polythiophenes, and TCTA, NPD, and TPT-TTF were chosen as additives to introduce carrier energy levels around the polymers for increased S. The dissimilar structures of the additives was also motivation for investigation, as they have different effects on polymer morphology and polymer-dopant interactions.

IV. Materials

1. High Mobility Bulk Polymers

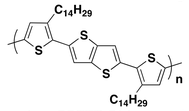

Fig. 4a. PBTTT-C14 has hole mobilities reaching up to 1 cm^2/Vs

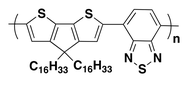

Fig. 4b. CDT-BTZ-C16 has hole mobilities reaching up to 5.5 cm^2/Vs

2. *p*-Type Dopants

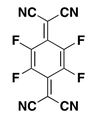

Fig. 5a. F_4TCNQ is mixed into the polymer solution before drop casting

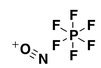

Fig. 5b. $NOPF_6$ was used as a dopant through polymer immersion

3. Small Molecule Additives

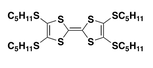

Fig. 6a. TPT-TTF

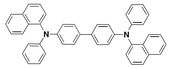

Fig. 6b. NPD

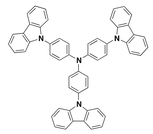

Fig. 6c. TCTA

4. HOMO and LUMO Energy Levels

The figure to the right shows the HOMO (the energy levels at the bottom of the bars) and LUMO (those at the top of the bars) levels for the various components being tested. PBTTT-C14 is predicted to form a charge transfer complex with F_4TCNQ; the dopant accepts an electron from the polymer, leaving behind a hole and increasing the number of charge carriers in the bulk.

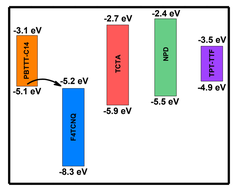

Fig. 7. HOMO and LUMO energy levels for materials of interest

V. Device Fabrication and Testing

The thermoelectric devices being tested for S and σ are shown. They are composed of a glass slide substrate with thermally evaporated Au electrodes and a drop casted polymer. The devices are tested using a Peltier module, a multimeter probe, and a thermocouple.

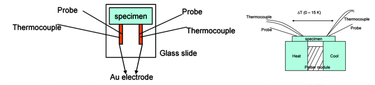

Fig 8. Thermoelectric device structure and testing setup

The thickness and film quality of the devices were evaluated using a 3D laser scanning microscope. The PBTTT-C14, F_4TCNQ, and TCTA system exhibited high quality films.

VI. Results

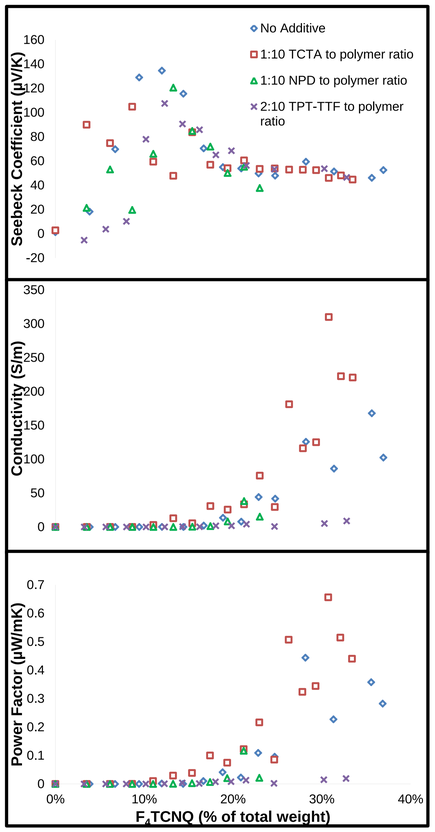

Fig 9. S, σ, and Power Factor vs F_4TCNQ concentration for no additive, 1:10 TCTA to polymer ratio, 1:10 NPD to polymer ratio, and 2:10 TPT-TTF to polymer ratio systems

S, σ, and Power Factor data was plotted as a function of F_4TCNQ concentration in PBTTT-C14. No additive, 1:10 TCTA to polymer ratio, 1:10 NPD to polymer ratio, and 2:10 TPT-TTF to polymer ratio systems were tested. All of the systems showed increasing, decreasing, and then plateauing S with increased F_4TCNQ concentration. Preliminary results suggest that TCTA shifts the S onset to lower dopant concentrations, while NPD and TPT-TTF shift the S onset to higher dopant concentrations. While σ increases with dopant level for all of the additive systems, the TCTA system appeared to have higher conductivities, while the TPT-TTF system had lower conductivities. Finally, TCTA appeared to have increased the Power Factor of the composites, while TPT-TTF decreased it. Differences in the highest Power Factors appear to be mainly a function of σ, as S levels off in the high dopant regimes.

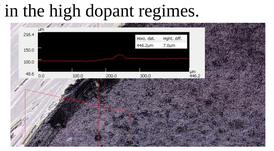

Fig. 10. 3D laser scanning microscope image of a scratched film, showing thickness and film quality

Another result was the successful synthesis and characterization of CDT-BTZ-C16, as described in the literature.

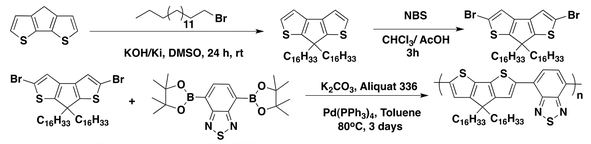

Fig 11. The synthesis of CDT-BTZ-C16

VII. Conclusions

It has been reported that a charge transfer complex may form due to the interaction of PBTTT-C14 and F_4TCNQ, and the trend of increasing σ with increased F_4TCNQ concentration supports this proposition. As seen in Fig. 7, an electron from the PBTTT-C14 HOMO level of -5.1 eV can assume lower energy by transferring to the F_4TCNQ LUMO level of -5.2 eV, leaving behind a hole in the polymer chain. With increasing concentrations of F_4TCNQ, additional charge carriers are introduced to the polymer, leading to higher σ. The result that the addition of TCTA increases the σ of these systems even further may be because it is acting as a stabilizer for the charge transfer complex between PBTTT-C14 and F_4TCNQ, enabling higher dopant saturation. The structure of the TCTA may also be conducive to improved morphology of the thin films, leading to increased σ.

VIII. Future Work

- Test devices with higher dopant concentrations and use $NOPF_6$
- Use different concentrations of TCTA
- Make nanostructured inorganic and organic composites
- Synthesize CDT-BTZ-C16 in bulk and repeat the experiment for the higher mobility polymer
- Find another polymer with high known conductivity and work backwards from the high conductivity state

References

(a) Sun, J.; Yeh, M.; Jung, B. J.; Zhang, B.; Feser, J.; Majumdar, A.; Katz, H. E. *Macromolecules* **2010**, *43*, 2897; (b) Kong, H.; Jung, B. J.; Sinha, J.; Katz, H. E. *Chem. Mater.* **2012**, *24*, 2621; (c) Sinha, J.; Lee, S. J.; Kong, H.; Swift, T. W.; Katz, H. E. *Macromolecules* **2013**, *46*, 708; (d) Sinha, J.; Ireland, R. M.; Lee, S. J.; Katz, H. E. *MRS Commun.* **2013**, *1;* (e) Snyder, G. J.; Toberer, E. S. *Nat. Mater.* **2008**, *7*, 105; (f) Poehler, T. O.; Katz, H. E. *Energy Environ. Sci.* **2012**, *5*, 8110; (g) Zhang, B.; Sun, J.; Katz, H. E.; Fang, F.; Opila, R. L. *ACS Appl. Mater. Interfaces* **2010**, *2*, 3170; (h) Zhang, M.; Tsao, H.; Yang, C.; Mishra, A. K., Müllen, K. *J. Am. Chem. Soc.* **2007**, *129*, 3473; (i) Lawrence Livermore National Laboratory 2012

Acknowledgements

Thanks to Dr. Orla Wilson for research guidance, Dr. Weiguo Huang for help with Au evaporation, and Ming-Ling Yeh for design advice. Funding from the JHU Office of the Provost through a 2012 PURA Grant.